

# Improving Bone Microarchitecture in Aging with Diosgenin Treatment: A Study in Senescence-Accelerated OXYS Rats

Maria A. Tikhonova<sup>1,\*</sup>, Che-Hao Ting<sup>2</sup>, Nataliya G. Kolosova<sup>3</sup>, Chao-Yu Hsu<sup>4</sup>,  
Jian-Horng Chen<sup>5</sup>, Chi-Wen Huang<sup>6</sup>, Ging-Ting Tseng<sup>7</sup>, Ching-Sui Hung<sup>8,\*</sup>,  
Pan-Fu Kao<sup>6,9</sup>, Tamara G. Amstislavskaya<sup>1</sup>, and Ying-Jui Ho<sup>10</sup>

<sup>1</sup>Laboratory of Evolutionary Genetics, Institute of Cytology and Genetics SB RAS, Novosibirsk 630090, Russia

<sup>2</sup>School of Dentistry, Chung Shan Medical University, Taichung 40201

<sup>3</sup>Department of Molecular Mechanisms of Ageing, Institute of Cytology and Genetics SB RAS, Novosibirsk 630090, Russia

<sup>4</sup>Division of Urology, Department of Surgery, Tungs' Taichung Metrohabor Hospital, Taichung 43503

<sup>5</sup>School of Physical Therapy, Chung Shan Medical University, Taichung 40201

<sup>6</sup>Molecular Imaging Laboratory, Department of Nuclear Medicine, Chung Shan Medical University Hospital, Taichung 40201

<sup>7</sup>School of Medical Laboratory and Biotechnology, Chung Shan Medical University, Taichung 40201

<sup>8</sup>Occupational Safety and Health Office, Department of Education and Research Taipei City Hospital, Taipei 10341

<sup>9</sup>School of Medicine, Chung Shan Medical University, Taichung 40201  
and

<sup>10</sup>School of Psychology, Chung Shan Medical University Hospital, Chung Shan Medical University Taichung 40201, Taiwan, Republic of China

## Abstract

Osteoporosis is a major disease associated with aging. We have previously demonstrated that diosgenin prevents osteoporosis in both menopause and D-galactose-induced aging rats. OXYS rats reveal an accelerated senescence and are used as a suitable model of osteoporosis. The aim of the present study was to analyze microarchitecture and morphological changes in femur of OXYS rats using morphological tests and microcomputed tomography scanning, and to evaluate the effects of oral administration of diosgenin at 10 and 50 mg/kg/day on femur in OXYS rats. The result showed that, compared with age-matched Wistar rats, the femur of OXYS rats revealed lower bone length, bone weight, bone volume, frame volume, frame density, void volume, porosity, external and internal diameters, cortical bone area, BV/TV, Tb.N, and Tb.Th, but higher Tb.Sp. Eight weeks of diosgenin treatment decreased porosity and Tb.Sp, but increased BV/TV, cortical bone area, Tb.N and bone mineral density, compared with OXYS rats treated with vehicle. These data reveal that microarchitecture and morphological

Corresponding authors: [1] Ying-Jui Ho, Ph.D., School of Psychology, Chung Shan Medical University Hospital, Chung Shan Medical University, No. 110, Sec. 1, Jianguo N. Rd., Taichung City 40201, Taiwan, R.O.C. Tel: +886-4-24730022 ext. 11858, Fax: +886-4-23248191, E-mail: yjho@csmu.edu.tw; joshuayjho@gmail.com; [2] Pan-Fu Kao, Ph.D., Molecular Imaging Laboratory, Department of Nuclear Medicine, Chung Shan Medical University Hospital; School of Medicine, Chung Shan Medical University, No. 110, Sec. 1, Jianguo N. Rd., Taichung City 40201, Taiwan, R.O.C. Tel: +886-4-24730022 ext. 32077, E-mail: pfkao@csmu.edu.tw; and [3] Tamara G. Amstislavskaya, Ph.D., Sc.D., Laboratory of Evolutionary Genetics, Institute of Cytology and Genetics SB RAS, Pr. Lavrentjeva, 10, Novosibirsk, 630090, Russia. Tel: +7-383-335-98-01, Fax: +7-383-335-97-54, E-mail: amstislavskaya@yandex.ru

\*Contributed to this work equally.

Received: September 27, 2014; Revised: December 1, 2014; Accepted: December 31, 2014.

©2015 by The Chinese Physiological Society and Airiti Press Inc. ISSN : 0304-4920. <http://www.cps.org.tw>

changes in femur of OXYS rats showed osteoporotic aging features and suggest that diosgenin may have beneficial effects on aging-induced osteoporosis.

**Key Words:** aging, bone loss, diosgenin, microcomputed tomography, osteoporosis, OXYS rats

## Introduction

Osteoporosis is one of the most prevalent and serious diseases in the elderly. Aging-induced osteoporosis is associated with a reduction in mineralization and increase in porosity in the cortical and trabecular bones, which results in bone loss and increased risk of fracture. Oxidative stress has been proposed as a major cause of aging (46, 56) and age-related bone loss (62).

Laboratory rodents are the most convenient animal models for osteoporosis research (36), but there are only a few examples of rodent genetic models of osteoporosis. Over the last few years, a large amount of experimental data has demonstrated that accelerated senescent OXYS rats are a suitable model of osteoporosis. OXYS rats were produced in the Institute of Cytology and Genetics of the SB Russian Academy of Sciences (Novosibirsk, Russia) by selective breeding of Wistar rats that were highly sensitive to the cataractogenic effect of D-galactose (51). These rats develop early spontaneous cataracts and degenerative features that are regarded as syndromes of accelerated senescence (33). OXYS rats have a shortened lifespan and show early development of age-related pathological phenotypes similar to geriatric disorders observed in humans, including senile osteoporosis (41), cataracts, retinopathy (42, 64), and signs of accelerated aging (31, 44). These features make it possible to use OXYS rats to evaluate the efficacy of treatments for osteoporosis. Thus, detailed analysis of microarchitecture and morphological changes in the bone of OXYS rats is needed. Furthermore, OXYS rats have low glutathione levels, high malondialdehyde (MDA) levels, and high superoxide dismutase (SOD) activities (50). Recently, some aging-related features of OXYS rats were found to be corrected or improved by supplementation with anti-oxidants (4, 32, 45, 53). Therefore, OXYS rats are useful for detecting effects of anti-oxidant drugs on osteoporosis.

Antioxidants scavenge free radicals and protect cells and organs from oxidative damage. Among the natural antioxidants, dioscorea (wild yam) is noteworthy. Dioscorea, a common food and Chinese medicine (40), contains phytosteroids, such as diosgenin and steroidal saponins (19), and has long been used to treat menopausal syndrome and has anti-osteoporotic activities (10, 61). Dioscorea also decreases inflammatory cytokine levels in the brain of menopausal rats (22). Diosgenin, the main steroidal saponin in di-

oscorea, has a chemical structure similar to steroid hormones, and is used as a precursor in the manufacture of estrogen, progesterone, testosterone and cortisol (17, 49). In addition, it has antioxidant and free radical scavenging activities in rats (12, 52), shows anti-aging effects in menopausal animals (21), improves epidermal functions in aging mice (54). Diosgenin also improves learning and memory in a D-galactose-induced aging model in mice (12).

Three-dimensional (3D) microcomputed tomography ( $\mu$ CT) scanning has been used for more than a decade to examine microarchitecture of bone with high accuracy (16), to evaluate osteoporosis and bone disease (7, 29, 57), and to characterize trabecular bone in patients with hyperparathyroidism and osteoporosis (13).  $\mu$ CT provides 3D images of high resolution ( $\sim 9 \mu\text{m}$ ), making it possible to visualize trabecular microstructure that previously could only be assessed using bone biopsy samples, and to obtain morphometric measurements such as trabecular number (Tb.N), thickness (Tb.Th), and separation (Tb.Sp), bone volume (BV), trabecular tissue volume (TV), and bone volume fraction (BV/TV) (20).

Microarchitecture of bone in OXYS rats has not yet been examined, and it is not known whether diosgenin affects the bone of OXYS rats. The aim of the present study was to use  $\mu$ CT to examine microarchitecture of the femur of OXYS rats, and to elucidate the effects of diosgenin, at 10 or 50 mg/kg/day, on the femur.

## Materials and Methods

### *Animals and Drug Administration*

Twelve-week-old male OXYS rats (weighing  $268.0 \pm 4.9 \text{ g}$ ,  $n = 29$ ), obtained from the Institute of Cytology and Genetics, Russian Academy of Sciences, Russia, and the same age male Wistar rats (weighing  $416.2 \pm 9.8$ ,  $n = 8$ , used as health control) were housed in groups of four or five in acrylic cages ( $35 \times 56 \times 19 \text{ cm}$ ) in an animal room with a 12 h light-dark cycle (lights on at 07:00 h) with food and water available *ad libitum*. The OXYS rats were divided into three experimental groups: aging control rats ( $n = 10$ ), or rats treated with diosgenin at a dose of 10 mg/kg/day ( $n = 10$ ) or 50 mg/kg/day ( $n = 9$ ). All experimental procedures were performed according to the NIH Guide for the Care and Use of Laboratory Animals and were approved by the Animal Care Committee of Chung Shan Medical University (IACUC approval No.: 1018). All

efforts were made to minimize the number of animals used and their suffering.

**General Procedure:** Starting at 12 weeks of age (day 0), the OXYS rats underwent diosgenin treatment (0, 10 or 50 mg/kg/day, p.o.) for 8 weeks. The Wistar control rats received the vehicle. All the rats were sacrificed on day 57 by exposure to CO<sub>2</sub>, and the femur bones dissected out, frozen and stored at -70°C until use.

**Drugs and Drug Administration:** Diosgenin was purchased from Sigma-Aldrich (St. Louis, MO, USA). An appropriate amount (see below) of the drug was mixed with flour and water to produce 0.8 g pellets. One pellet was given per day to each rat at 12:00-13:00 h for 56 days; the control rats received pellets without the drug. The body weight of each rat was measured daily, then the pellet mixture for that day was prepared individually for each rat based on its body weight.

#### *Preparation of Femora and Determination of the Morphometric Properties*

During the removal of the muscle and the fibrous periosteum, the femora were kept wet using distilled water. After defatting in chloroform and drying, the right femur was used to sequentially measure the morphometric parameters of wet weight, total volume, dry weight, and frame volume, which were then used to calculate the void volume and porosity.

**Measurement of the Wet Weight:** The femur was placed in an unstoppered glass vial containing distilled water. The vial was then placed in a vacuum desiccator for 90 min to remove air diffusing out of the bone (25). After gently wiping off the water on the surface of the specimen, the femur was weighed using an analytical balance to obtain the wet weight ( $W_W$ ).

**Measurement of the Total Volume:** According to the theory of porous media (6), the porous structure of the bone consists of the 'solid skeleton' (bone frame volume;  $V_F$ ) and the 'interstitial fluid' (void volume;  $V_V$ ) (58). Instead of using conventional calipers or mathematical equations, we have, by combining Newton's third law and Archimedes' principle, developed a novel and accurate method for directly measuring the total volume ( $V_T$ ;  $V_T = V_F + V_V$ ; cm<sup>3</sup>) of the femur (38, 59). Briefly, each right femur was suspended by a thin silk yarn and fully immersed in water in a beaker on an analytical balance and the buoyant force ( $\bar{B}$ ; g) was read directly from the balance display. The total volume,  $V_T$ , of the femur was calculated as  $V_T = \bar{B}/0.9971$ , where 0.9971 is the density (in g/cm<sup>3</sup>) of distilled water at 25°C and 1 atmosphere (65).

**Measurement of the Dry Weight:** After measuring the total volume, each right femur was placed in an

incubator at 50°C for 72 h to remove the interstitial fluid until a constant weight (< 0.05% change) was obtained when weighed at 1 h intervals, then the dry weight ( $W_D$ ) was immediately measured on an analytical balance.

**Calculation of the Morphometric Parameters:** Bone porosity was calculated as follows. In the saturated right femur, the void space was filled with  $W_F$  g of distilled water. The void volume,  $V_V$ , was calculated using the equations  $V_V = W_F / 0.9971$  and  $W_F = W_W - W_D$ ; the porosity,  $P$ , was calculated using the equation  $P = V_V / V_T$ .

#### *Measurement of the Trabecular Structure by $\mu$ CT*

The femur was analyzed by  $\mu$ CT (Skyscan 1176, SKYSCAN, Belgium) without further sample preparation. Sequential transaxial images through the distal half of the femoral shaft were obtained using an isotropic voxel size of 9  $\mu$ m, current of 500  $\mu$ A, exposure time of 1,000 ms, peak tube voltage of 50 kV, and a 0.5 mm aluminum filter. The scanning angular rotation was 180 degrees in angular increments of 0.5 degrees. Data sets were reconstructed using the software provided with the equipment (Skyscan™ NRecon software, version 1.6.9.3) and segmented into binary images (16-bit BMP images). To analyze the micro-architectural properties of the trabecular bones, volumes of interest (VOIs) in the femur were evaluated. For analyzing the trabecular bone, a VOI was selected starting 0.45 mm (50 image slices) from the growth plate (GP) and extending a longitudinal distance of 3.60 mm in the proximal direction (400 image slices analyzed, cortical bone excluded), while, for an image slice, taken at the middle of the bone, was used for analyzing the cortical bone (Fig. 1).

Regions of interest in the trabecular and cortical bone were obtained by manual drawing on the scanned image and analyzed using the software provided with the equipment (Skyscan™ CT-analyzer software, version 1.6.0). Morphometric indices of the trabecular bone region were determined from the micro-tomographic data sets (integrated over a VOI) using direct 3D morphometry. The total volume of the VOI (tissue volume  $TV$ , mm<sup>3</sup>) and the trabecular bone volume ( $BV$ ; mm<sup>3</sup>) were calculated based on the hexahedral marching cubes volume model of the VOI. The  $BV/TV$  (%) was then calculated. The  $Tb.Th$  ( $\mu$ m),  $Tb.Sp$  ( $\mu$ m),  $Tb.N$  (mm<sup>-1</sup>) and bone mineral density (BMD) were obtained by image analysis.

Tomographic scans were performed *ex vivo* on the excised femur as described above. Each pixel of the reconstructed 8-bit BMP image had a color or grey value between 0 and 255. A grey value of 255 was assumed to be white (void space), whereas a value of 0 was taken as black or the densest part of the image.

**Table 1. Effects of diosgenin on the morphological properties of the femur in OXYS rats.**

	Wistar	OXYS		
	Vehicle (n = 8)	Vehicle (n = 10)	Diosgenin 10 mg/kg/day (n = 10)	Diosgenin 50 mg/kg/day (n = 9)
Bone length	39.95 ± 0.29	36.52 ± 0.17***	36.76 ± 0.17***	35.99 ± 0.18***
Dry weight (g)	0.80 ± 0.02	0.53 ± 0.01***	0.54 ± 0.01***	0.49 ± 0.01***, #
Wet weight (g)	1.02 ± 0.02	0.65 ± 0.02***	0.64 ± 0.02***	0.58 ± 0.03***, ##
Bone volume (cm <sup>3</sup> )	0.66 ± 0.01	0.46 ± 0.01***	0.46 ± 0.02***	0.42 ± 0.02***, #
Frame volume (cm <sup>3</sup> )	0.44 ± 0.01	0.34 ± 0.01***	0.35 ± 0.02***	0.33 ± 0.01***
Frame density (g/cm <sup>3</sup> )	1.82 ± 0.02	1.58 ± 0.03***	1.55 ± 0.04***	1.50 ± 0.04***

\*\*\* $P < 0.001$  compared to the Wistar controls, # $P < 0.05$ , ## $P < 0.01$ , compared to OXYS rats treated with vehicle. Data are expressed as the mean ± SEM.

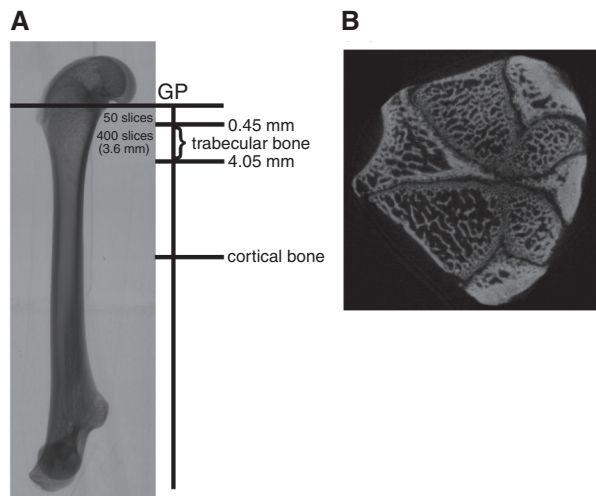


Fig. 1. Bone image obtained by  $\mu$ CT scanning. In (A), the level of the growth plate (GP) and the bone area and image number used for analyzing trabecular and cortical bone are indicated. (B) is a cross-section of the bone from the GP.

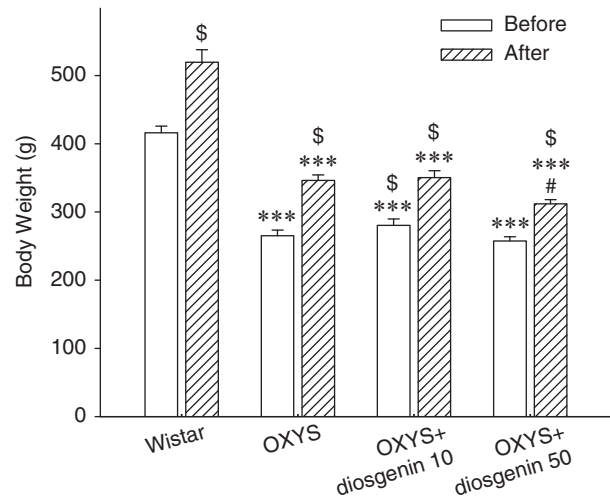


Fig. 2. Body weight of the rats before and after 8 weeks of diosgenin treatment. The dosages of diosgenin were 10 and 50 mg/kg/day. \*\*\* $P < 0.001$  compared to the Wistar control. # $P < 0.05$  compared to the OXYS rats treated with vehicle. \$ $P < 0.001$  compared with the body weight before the experiment. Data are expressed as the mean ± SEM.

### Statistical Analysis

One-way ANOVA, followed by the least-significant difference (LSD) *post hoc* test, was used to evaluate differences between the groups. A test of homogeneity of the variances of the parameters measured showed no significance (values of Levene statistic > 0.598), indicating that the differences in sample size between the groups did not affect the statistical results. All results are expressed as the mean ± SEM. The level of significance was defined as  $P < 0.05$ .

### Results

The OXYS rats showed lower body weight than the control Wistar rats before and after the experiment ( $F(3,36) > 69.28$ ,  $P < 0.001$ ). Paired-samples  $t$  test revealed that all the rats showed higher body weight at

the end of the experiment, compared with that before the experiment (all  $t$ -values > 7.05, all  $P$ -values < 0.001). Diosgenin treatment, at the dose of 50 mg/kg/day, significantly decreased the body weight, compared with the OXYS rats treated with vehicle ( $P < 0.05$ ) (Fig. 2). However, the percentage of body weight changes, which ranged from  $21.4 \pm 2.6\%$  to  $31.7 \pm 5.3\%$ , did not show between-group differences ( $F(3,36) = 1.18$ ,  $P = 0.33$ ). The ANOVA followed by LSD *post hoc* test revealed differences of morphological properties of femur between the groups, where bone length ( $F(3,36) = 71.49$ ,  $P < 0.001$ ), dry weight ( $F(3,36) = 100.58$ ,  $P < 0.001$ ), wet weight ( $F(3,36) = 115.46$ ,  $P < 0.001$ ), bone volume ( $F(3,36) = 46.17$ ,  $P < 0.001$ ), frame volume ( $F(3,36) = 15.22$ ,  $P < 0.001$ ), and frame density ( $F(3,36) = 13.09$ ,  $P < 0.001$ ) of OXYS rats were significantly lower than those in the Wistar rats



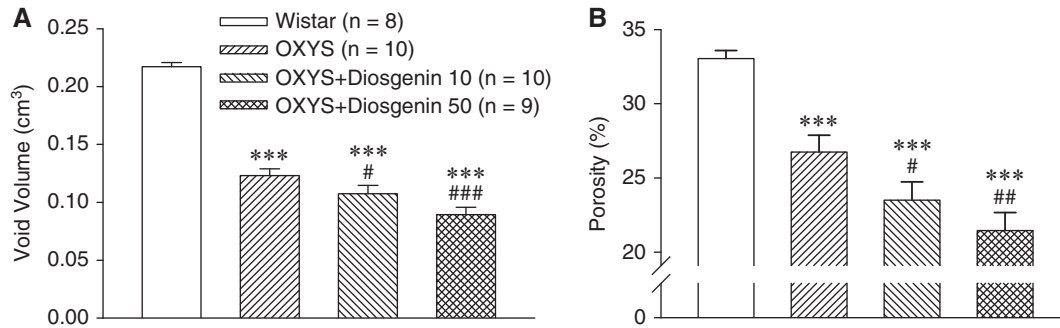


Fig. 3. Effects of diosgenin on the morphological properties of the femur in OXYS rats. (A) Void volume; (B) porosity. \*\*\* $P < 0.001$  compared to the Wistar control. # $P < 0.05$ , ## $P < 0.01$ , ### $P < 0.001$  compared to the OXYS rats treated with vehicle. Data are expressed as the mean  $\pm$  SEM.

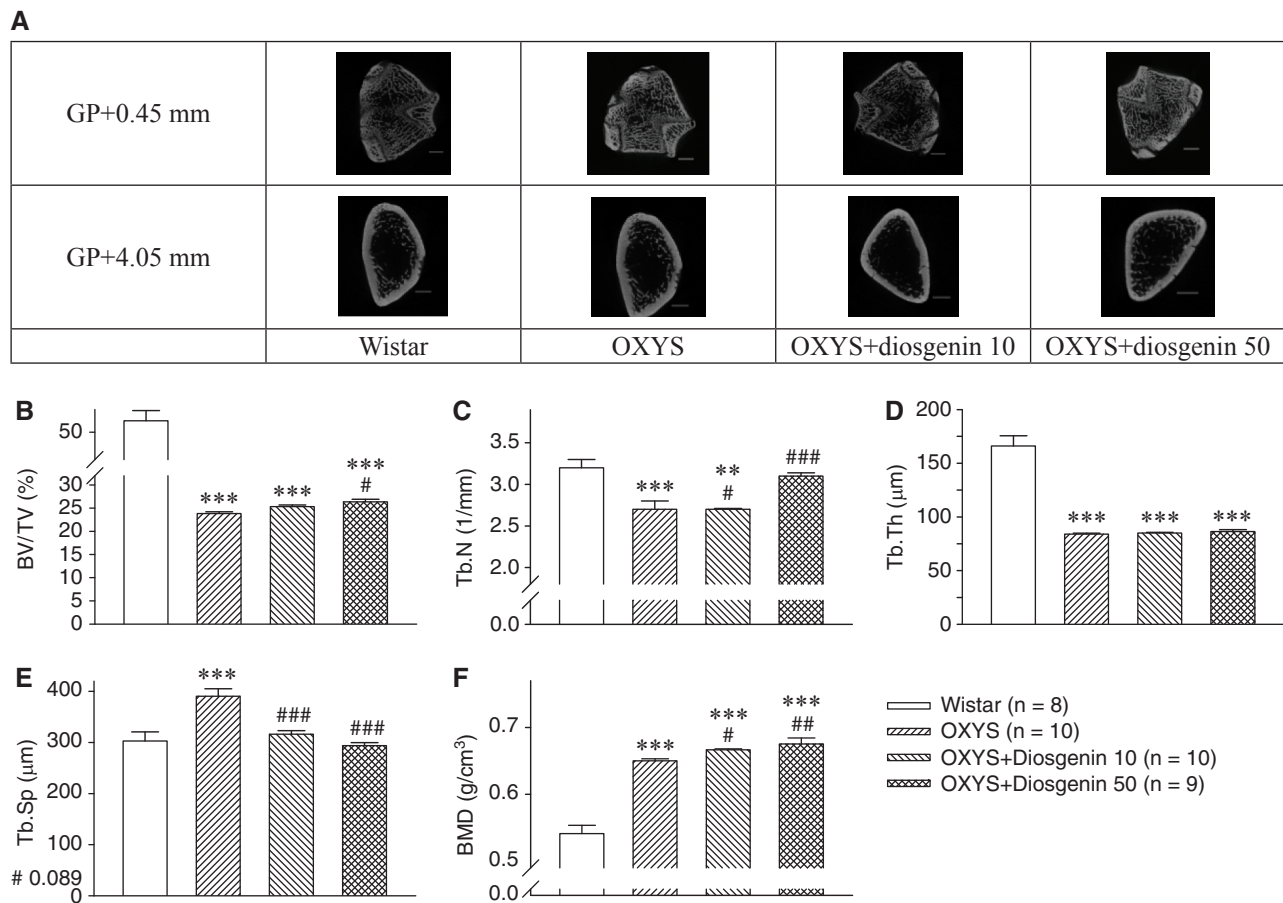


Fig. 4. Effects of diosgenin on the microarchitecture of femur in OXYS rats analyzed by  $\mu$ CT. (A) The images in the upper panel were taken at the level 0.45 mm below the growth plate (GP). The images in the lower panel were taken 4.05 mm below the GP. The images between the upper and lower panels (400 image slices) were used for analyzing trabecular microarchitecture; bar, 1 mm. The figure illustrates: bone volume fraction (BV/TV) (B), trabecular number (Tb.N) (C), trabecular thickness (Tb.Th) (D), trabecular separation (Tb.Sp) (E) and bone mineral density (BMD) (F). \*\* $P < 0.01$  and \*\*\* $P < 0.001$  compared to the Wistar control. # $P < 0.08$ , ## $P < 0.01$ , ### $P < 0.001$  compared to the OXYS rats treated with vehicle. Data are expressed as the mean  $\pm$  SEM.

(estimate of effect size, all partial Eta squared  $> 0.54$ ). Chronic administration of diosgenin at the dosage of 50 mg/kg/day, but not 10 mg/kg/day, resulted in a significant decrease in dry weight, wet weight and bone

volume (all  $P$ -values  $< 0.05$ ), compared with the OXYS rats treated with vehicle (Table 1).

The void volume ( $F(3,36) = 79.24$ ,  $P < 0.001$ ) and porosity ( $F(3,36) = 19.15$ ,  $P < 0.001$ ) of the OXYS

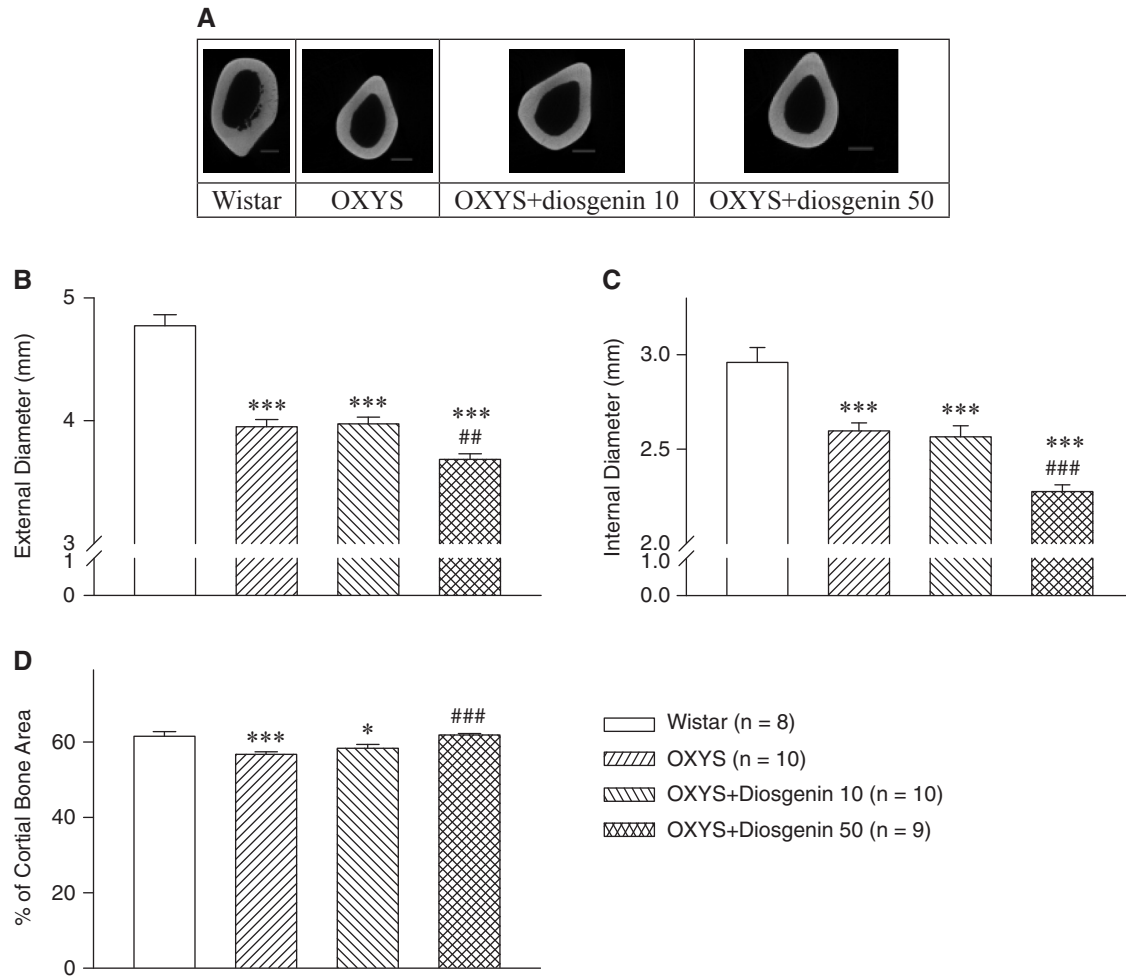


Fig. 5. Effects of diosgenin on the cortical bone of femur in OXYS rats analyzed by  $\mu$ CT. (A) The images, taken at the middle of the bone, were used for analyzing the cortical bone; bar, 1 mm. (B) external diameter, (C) internal diameter, (D) percentage of cortical bone area. \* $P < 0.05$  and \*\*\* $P < 0.001$  compared to the Wistar control. ### $P < 0.001$  compared to the OXYS rats treated with vehicle. Data are expressed as the mean  $\pm$  SEM.

rats were significantly lower than that in the Wistar rats. Diosgenin treatment, at the dosage of 10 and 50 mg/kg/day, decreased the void volume and porosity (both  $P$ -values  $< 0.05$ ) (Fig. 3).

Using the images obtained by  $\mu$ CT, the microarchitecture of the cortical bone and trabecular bone of the femur was analyzed. The images used for analyzing BV, TV and trabecular parameters are shown in Fig. 4A. The TV, BV ( $F(3,36) > 12.329$ ,  $P < 0.001$ ) (data not shown), BV/TV (Fig. 4B), Tb.N ( $F(3,36) = 11.57$ ,  $P < 0.001$ , partial Eta squared = 0.51) (Fig. 4C), and Tb.Th ( $F(3,36) = 86.62$ ,  $P < 0.001$ , partial Eta squared = 0.89) (Fig. 4D) of the OXYS rats were significantly lower than that in the Wistar rats. The OXYS rats showed higher Tb.Sp ( $F(3,36) = 13.74$ ,  $P < 0.001$ , partial Eta squared = 0.56) (Fig. 4E) and BMD ( $F(3,36) = 98.79$ ,  $P < 0.001$ , partial Eta squared = 0.90) (Fig. 4F), compared to that in the Wistar rats. Diosgenin did not affect the TV, BV (data not shown), and Tb.Th. How-

ever, diosgenin at 50 mg/kg/day slightly increased the BV/TV ( $P = 0.089$ ) (Fig. 4B). Diosgenin, at both 10 and 50 mg/kg/day, significantly increased the Tb.N (both  $P$ -values  $< 0.05$ ) (Fig. 4C) and BMD (both  $P$ -values  $< 0.01$ ) (Fig. 4F) but reduced the Tb.Sp (both  $P$ -values  $< 0.001$ ) in a dose-dependent manner (Fig. 4E).

The images used for analyzing bone diameter and cortical bone area are shown in Fig. 5A. OXYS rats revealed lower external diameter ( $F(3,36) = 51.92$ ,  $P < 0.001$ ) (Fig. 5B), internal diameter ( $F(3,36) = 23.73$ ,  $P < 0.001$ ) (Fig. 5C) and percentage of cortical bone area ( $F(3,36) = 8.10$ ,  $P < 0.001$ ) (Fig. 5D), compared with the Wistar control. Diosgenin treatment, at the dosage of 50 mg/kg/day, decreased the external diameter and internal diameter (both  $P$ -values  $< 0.01$ ), but increased the percentage of cortical area ( $P < 0.001$ ), compared with the OXYS rats treated with vehicle (Fig. 5). Femur microarchitecture of the animals is shown in Fig. 6.

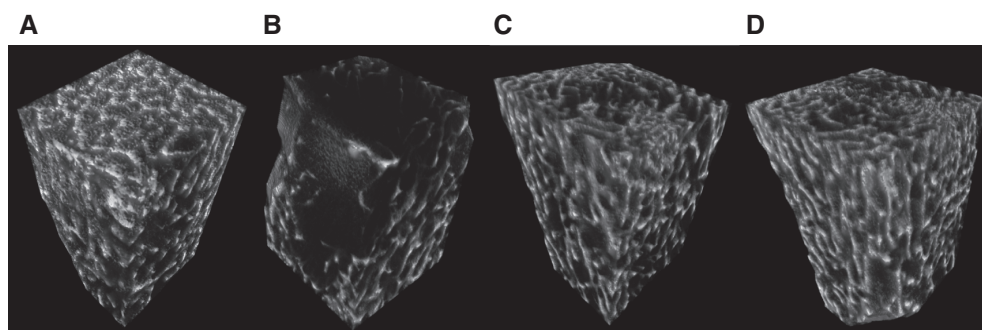


Fig. 6. Effects of diosgenin on the trabecular bone of the femur in OXYS rats. The figure shows a representative 3D architecture measured using  $\mu$ CT for (A) a Wistar control rat, (B) an OXYS rat treated with vehicle, (C) and (D) OXYS rats treated with diosgenin at 10 or 50 mg/kg/day, respectively.

## Discussion

Morphological and  $\mu$ CT image analysis of the femur revealed that OXYS rats show lower bone length, bone weight, bone volume, frame volume, frame density, void volume, porosity, external and internal diameters, percentage of cortical bone area, BV/TV, Tb.N and Tb.Th, but higher Tb.Sp, compared with the Wistar control. Eight weeks of diosgenin treatment decreased porosity and Tb.Sp, but increased BV/TV, cortical bone area and Tb.N, compared with the OXYS rats treated with vehicle. We also found that the BV/TV was positively correlated with the Tb.N ( $r = 0.817$ ) and negatively correlated with the Tb.Sp ( $r = -0.555$ ) (data not shown). This is the first study thoroughly examining microarchitecture and morphological changes in the femur of OXYS rats. The smaller physical size of OXYS femur is parallel to their smaller body size and weight. The bone features observed in OXYS rats are similar with that in menopausal rats (24) and in human (43). Treatment with diosgenin improved trabecular and cortical structure of the femur, suggesting that diosgenin has potential for the treatment of osteoporosis during aging.

An antioxidative action may be one of the mechanisms by which diosgenin decreases bone loss in OXYS rats. Accelerated senescence OXYS rats show aging features, including osteoporosis, cognitive deficit, reproductive dysfunction and neurodegeneration as early as 3 months of age (2, 34), and have high levels of free radicals (32) and oxidative damage to DNA and proteins in liver mitochondria and cytosol (26, 27, 30). We, therefore, propose that oxidative damage may play a role in the bone loss seen in the OXYS aging rat model. Diosgenin, one of the important bioactive ingredients in *Dioscorea*, has antiaging and antioxidant activities (39). A previous study reported that administration of diosgenin to D-galactose-induced senescent mice increases SOD and glutathione peroxidase activities and decreases MDA levels, suggesting that

diosgenin has beneficial effects on aging and oxidative stress-related disorders (12). Similarly, our previous study (10) has demonstrated that *Dioscorea* improves morphometric and mechanical properties of bone in menopausal animals. Our recent report (55) also showed an increase in sperm motility in aging rats after diosgenin treatment at the dosages of 10 and 50 mg/kg/day. Decreasing male motility of spermatozoa with aging is usually associated with oxidative stress due to accumulated seminiferous tubule damage (11).

Decreased blood levels of some sex hormones are also involved in osteoporosis. Postmenopausal women have low estrogen levels and exhibit osteoclast activation and increased risk of fracture and osteoporosis (35), and bone loss in these women can be prevented using estrogen (9). Lower serum androgen levels have been reported in idiopathic osteoporosis in males, and androgen has anabolic effects on bone and increases its mineral density (18). In addition, decreased levels of testosterone or dehydroepiandrosterone sulfate are seen in D-galactose-induced aging models in rats (63). Diosgenin has a similar chemical structure to sex hormones and has long been used as a precursor in the manufacture of steroid hormones, such as estrogen, progesterone, testosterone and cortisol (17, 49). Although nothing is known about the pathways by which diosgenin is converted into other hormones *in vivo*, chronic administration of diosgenin to rats has been found to increase progesterone levels (8) and reverse menopause-induced hypertrophy of the adrenal gland (5). Recovery of sex hormone levels have also been observed in postmenopausal women (60) and ovariectomized rats (8) treated with diosgenin. In addition, diosgenin can enhance bone formation by stimulating the synthesis and secretion of bone marker proteins, which increase the formation of  $\text{Ca}^{2+}$  deposits in the extracellular matrix, thereby increasing bone formation (3). Interestingly, it is known that diosgenin enhances formation of osteoprogenitor cells *in vitro* in the bone marrow (47). These

data lead us to suggest that the effects of diosgenin on bone loss in OXYS rats may, at least partially, attribute to its effects on hormonal systems and protein synthesis. Further studies are needed to address this issue.

Bone quality is related to its mechanical and morphological properties, which determine fracture risk. The lowered Tb.N and higher Tb.SP in OXYS rats is similar to the trabecular bone loss in the osteoporotic rat model (24). In the present study, 2 months of diosgenin administration resulted in significant increases in BV/TV, cortical bone area and Tb.N and significant decreases in void volume, porosity, and Tb.Sp. Higher bone porosity has been correlated with increased risk of fracture (14, 15). Further, an improvement of cortical component was seen after effective anti-osteoporotic therapy (24). Thus, the above diosgenin-induced bone changes may increase bone quality.

The trabecular microarchitecture also contributes to bone strength. 3D  $\mu$ CT and high resolution peripheral quantitative computer tomography analysis of the same bone biopsy has shown that trabecular architecture contributes to bone strength (13). Thus, assessment of trabecular architecture using  $\mu$ CT can predict fracture. A correlation has been found between morphological parameters of the femur, such as Tb.Sp, Tb.N and BV/TV, and mechanical properties, such as failure load and stiffness (37). Other studies have suggested that the Tb.Sp is an important determinant of bone strength. A  $\mu$ CT study of bone reported that women with documented vertebral fractures showed a 49% increase in the Tb.Sp compared to women without vertebral fractures (28). Similarly, in a study comparing 2D histomorphometry and 3D  $\mu$ CT parameters in Japanese women with or without spinal fractures (23), the Tb.N was significantly lower and the Tb.Sp significantly higher in those with spinal fractures. Furthermore, thinning of trabeculae has been documented in steroid-induced osteoporosis, which increases the risk of fracture (1). The present study did not find any change in the Tb.Th but revealed an increase in Tb.N after diosgenin treatment. In addition, decreases in the Tb.Sp, void volume and porosity were observed after diosgenin treatment, showing that diosgenin increases trabecular number and density, but not trabecular thickness. These changes may, therefore, increase the mechanical strength. There is evidence that when bone loss occurs in osteoporosis, trabecular bone is affected at an earlier date and more severely than cortical bone (24, 37). Interestingly, our data showed that diosgenin enhanced not only Tb.N but also cortical bone area. Further investigations are needed on the effect of diosgenin on mechanical properties.

In conclusion, the present study showed microarchitecture and morphological changes in the femur

of OXYS rats, and indicated that the bone of OXYS rats reveals osteoporotic features. Our data demonstrate that extended administration of diosgenin to OXYS rats increases the BV/TV, cortical bone area, Tb.N and BMD, and decreases Tb.Sp, void volume and porosity. This study suggests that diosgenin may have potential in the treatment of aging-induced osteoporosis. By using the body surface area normalization method (48), the effective dose, 50 mg/kg/day, of diosgenin in improving bone quality in rats can be translated to the human equivalent dose of 8.1 mg/kg/day. Further studies are needed to determine the optimal and safe dose for elderly.

### Acknowledgments

This work was supported by grants from the Ministry of Science and Technology (MOST 103-2410-H-040-002-MY2 and MOST 104-2923-H-040-001-MY3) and National Science Council of the ROC (NSC 102-2410-H-040-004 and NSC 100-2923-H-040-009-MY3) and by budget project No. VI.53.2.4. of the Institute of Cytology and Genetics SB RAS.

### Conflicts of Interest

The authors declare no conflicts of interest for the material in the manuscript.

### References

1. Aaron, J.E., Francis, R.M., Peacock, M. and Makins, N.B. Contrasting microanatomy of idiopathic and corticosteroid-induced osteoporosis. *Clin. Orthop. Relat. Res.* 243: 294-305, 1989.
2. Agafonova, I.G., Kotelnikov, V.N., Mischenko, N.P. and Kolosova, N.G. Evaluation of effects of histochrome and mexidol on structural and functional characteristics of the brain in senescence-accelerated OXYS rats by magnetic resonance imaging. *Bull. Exp. Biol. Med.* 150: 739-743, 2011.
3. Alcantara, E.H., Shin, M.Y., Sohn, H.Y., Park, Y.M., Kim, T., Lim, J.H., Jeong, H.J., Kwon, S.T. and Kwun, I.S. Diosgenin stimulates osteogenic activity by increasing bone matrix protein synthesis and bone-specific transcription factor Runx2 in osteoblastic MC3T3-E1 cells. *J. Nutr. Biochem.* 22: 1055-1063, 2011.
4. Amstislavskaya, T.G., Maslova, L.N., Gladkikh, D.V., Belousova, I.I., Stefanova, N.A. and Kolosova, N.G. Effects of the mitochondria-targeted antioxidant SkQ1 on sexually motivated behavior in male rats. *Pharmacol. Biochem. Behav.* 96: 211-216, 2010.
5. Benghuzzi, H., Tucci, M., Eckie, R. and Hughes, J. The effects of sustained delivery of diosgenin on the adrenal gland of female rats. *Biomed. Sci. Instrum.* 39: 335-340, 2003.
6. Biot, M.A. General theory of three-dimensional consolidation. *J. Appl. Phys.* 12: 155-164, 1941.
7. Buie, H.R., Campbell, G.M., Klinck, R.J., MacNeil, J.A. and Boyd, S.K. Automatic segmentation of cortical and trabecular compartments based on a dual threshold technique for *in vivo* micro-CT bone analysis. *Bone* 41: 505-515, 2007.
8. Chang, C.C., Kuan, T.C., Hsieh, Y.Y., Ho, Y.J., Sun, Y.L. and Lin, C.S. Effects of diosgenin on myometrial matrix metalloproteinase-2 and -9 activity and expression in ovariectomized rats. *Int. J. Biol. Sci.* 7: 837-847, 2011.



9. Checa, M.A., Del Rio, L., Rosales, J., Nogues, X., Vila, J. and Carreras, R. Timing of follow-up densitometry in hormone replacement therapy users for optimal osteoporosis prevention. *Osteoporos. Int.* 16: 937-942, 2005.
10. Chen, J.H., Wu, J.S.S., Lin, H.C., Wu, S.L., Wang, W.F., Huang, S.K. and Ho, Y.J. Dioscorea improves the morphometric and mechanical properties of bone in ovariectomized rats. *J. Sci. Food. Agric.* 88: 2700-2706, 2008.
11. Chen, S.J., Allam, J.P., Duan, Y.G. and Haidl, G. Influence of reactive oxygen species on human sperm functions and fertilizing capacity including therapeutical approaches. *Arch. Gynecol. Obstet.* 288: 191-199, 2013.
12. Chiu, C.S., Chiu, Y.J., Wu, L.Y., Lu, T.C., Huang, T.H., Hsieh, M.T., Lu, C.Y. and Peng, W.H. Diosgenin ameliorates cognition deficit and attenuates oxidative damage in senescent mice induced by D-galactose. *Am. J. Chin. Med.* 39: 551-563, 2011.
13. Cohen, A., Dempster, D.W., Muller, R., Guo, X.E., Nickolas, T.L., Liu, X.S., Zhang, X.H., Wirth, A.J., van Lenthe, G.H., Kohler, T., McMahon, D.J., Zhou, H., Rubin, M.R., Bilezikian, J.P., Lappe, J.M., Recker, R.R. and Shane, E. Assessment of trabecular and cortical architecture and mechanical competence of bone by high-resolution peripheral computed tomography: comparison with transiliac bone biopsy. *Osteoporos. Int.* 21: 263-273, 2010.
14. Cooper, C., Atkinson, E.J., O'Fallon, W.M. and Melton, L.J., 3rd. Incidence of clinically diagnosed vertebral fractures: a population-based study in Rochester, Minnesota, 1985-1989. *J. Bone Miner. Res.* 7: 221-227, 1992.
15. De Laet, C.E., van Hout, B.A., Burger, H., Hofman, A. and Pols, H.A. Bone density and risk of hip fracture in men and women: cross sectional analysis. *Brit. Med. J.* 315: 221-225, 1997.
16. Ding, M., Odgaard, A. and Hvid, I. Accuracy of cancellous bone volume fraction measured by micro-CT scanning. *J. Biomech.* 32: 323-326, 1999.
17. Djerassi, C. Drugs from Third World plants: the future. *Science* 258: 203-204, 1992.
18. Gillberg, P., Johansson, A.G. and Ljunghall, S. Decreased estradiol levels and free androgen index and elevated sex hormone-binding globulin levels in male idiopathic osteoporosis. *Calcif. Tissue Int.* 64: 209-213, 1999.
19. Hidaka, S., Okamoto, Y. and Arita, M. A hot water extract of *Chlorella pyrenoidosa* reduces body weight and serum lipids in ovariectomized rats. *Phytother. Res.* 18: 164-168, 2004.
20. Hildebrand, T., Laib, A., Muller, R., Dequeker, J. and Rueggsegger, P. Direct three-dimensional morphometric analysis of human cancellous bone: microstructural data from spine, femur, iliac crest, and calcaneus. *J. Bone Miner. Res.* 14: 1167-1174, 1999.
21. Ho, Y.J., Tai, S.Y., Pawlak, C.R., Wang, A.L., Cheng, C.W. and Hsieh, M.H. Behavioral and IL-2 responses to diosgenin in ovariectomized rats. *Chinese J. Physiol.* 55: 91-100, 2012.
22. Ho, Y.J., Wang, C.F., Hsu, W.Y., Tseng, T., Hsu, C.C., Kao, M.D. and Tsai, Y.F. Psychoimmunological effects of dioscorea in ovariectomized rats: role of anxiety level. *Ann. Gen. Psychiatry* 6: 21, 2007.
23. Ito, M., Nakamura, T., Matsumoto, T., Tsurusaki, K. and Hayashi, K. Analysis of trabecular microarchitecture of human iliac bone using microcomputed tomography in patients with hip arthrosis with or without vertebral fracture. *Bone* 23: 163-169, 1998.
24. Ito, M., Nishida, A., Koga, A., Ikeda, S., Shiraishi, A., Uetani, M., Hayashi, K. and Nakamura, T. Contribution of trabecular and cortical components to the mechanical properties of bone and their regulating parameters. *Bone* 31: 351-358, 2002.
25. Kalu, D.N., Masoro, E.J., Yu, B.P., Hardin, R.R. and Hollis, B.W. Modulation of age-related hyperparathyroidism and senile bone loss in Fischer rats by soy protein and food restriction. *Endocrinology* 122: 1847-1854, 1988.
26. Kemeleva, E.A., Sinitsyna, O.I., Conlon, K.A., Berrios, M., Kolosova, N.G., Zharkov, D.O., Vasyunina, E.A. and Nevinsky, G.A. Oxidation of guanine in liver and lung DNA of prematurely aging OXYS rats. *Biochemistry (Mosc)* 71: 612-618, 2006.
27. Kemeleva, E.A., Sinitsyna, O.I., Kolosova, N.G., Vasyunina, E.A., Zharkov, D.O., Conlon, K.A., Berrios, M. and Nevinsky, G.A. Immunofluorescent detection of 8-oxoguanine DNA lesions in liver cells from aging OXYS rats, a strain prone to overproduction of free radicals. *Mutat. Res.* 599: 88-97, 2006.
28. Kimmel, D.B., Recker, R.R., Gallagher, J.C., Vaswani, A.S. and Aloia, J.F. A comparison of iliac bone histomorphometric data in post-menopausal osteoporotic and normal subjects. *Bone Miner.* 11: 217-235, 1990.
29. Klinck, J. and Boyd, S.K. The magnitude and rate of bone loss in ovariectomized mice differs among inbred strains as determined by longitudinal *in vivo* micro-computed tomography. *Calcif. Tissue Int.* 83: 70-79, 2008.
30. Kolosova, N.G., Grishanova, A., Krysanova Zh, S., Zueva, T.V., Sidorova Iu, A. and Sinitsyna, O.I. Age-related changes in protein and lipid oxidation in the liver of prematurely aging rats OXYS. *Biomed. Khim.* 50: 73-78, 2004 [In Russian].
31. Kolosova, N.G., Kutorgin, G.D. and Safina, A.F. Bone mineralization in senescence-accelerated OXYS rats. *Bull. Exp. Biol. Med.* 133: 171-174, 2002.
32. Kolosova, N.G., Shcheglova, T.V., Sergeeva, S.V. and Loskutova, L.V. Long-term antioxidant supplementation attenuates oxidative stress markers and cognitive deficits in senescent-accelerated OXYS rats. *Neurobiol. Aging* 27: 1289-1297, 2006.
33. Kolosova, N.G., Stefanova, N.A. and Sergeeva, S.V. OXYS rats: a prospective model for evaluation of antioxidant availability in prevention and therapy of accelerated aging and age-related cognitive decline. In: Garipey, Q., and Menard, R. (eds.). *Handbook of Cognitive Aging: Causes, Proceses*. NY: Nova Science Publishers, 2009. pp. 47-82.
34. Kolosova, N.G., Vitovtov, A.O., Muraleva, N.A., Akulov, A.E., Stefanova, N.A. and Blagosklonny, M.V. Rapamycin suppresses brain aging in senescence-accelerated OXYS rats. *Aging (Albany NY)* 5: 474-484, 2013.
35. Legrand, E., Chappard, D., Pascaretti, C., Duquenne, M., Krebs, S., Rohmer, V., Basle, M.F. and Audran, M. Trabecular bone microarchitecture, bone mineral density, and vertebral fractures in male osteoporosis. *J. Bone Miner. Res.* 15: 13-19, 2000.
36. Lelovas, P.P., Xanthos, T.T., Thoma, S.E., Lyritis, G.P. and Dontas, I.A. The laboratory rat as an animal model for osteoporosis research. *Comp. Med.* 58: 424-430, 2008.
37. Lill, C.A., Gerlach, U.V., Eckhardt, C., Goldhahn, J. and Schneider, E. Bone changes due to glucocorticoid application in an ovariectomized animal model for fracture treatment in osteoporosis. *Osteoporos. Int.* 13: 407-414, 2002.
38. Lin, H.C., Wu, J.S.S., Hung, J.P., Yeh, W.C. and Chen, J.H. The study of positive correlation between bone frame mineral density and volume fraction in cortical bone. *J. Med. Biol. Eng.* 27: 136-142, 2007.
39. Liu, M.J., Wang, Z., Ju, Y., Wong, R.N. and Wu, Q.Y. Diosgenin induces cell cycle arrest and apoptosis in human leukemia K562 cells with the disruption of Ca<sup>2+</sup> homeostasis. *Cancer Chemother. Pharmacol.* 55: 79-90, 2005.
40. Liu, S.Y., Wang, J.Y., Shyu, Y.T. and Song, L.M. Studies on yams (*Dioscorea* spp.) in Taiwan. *J. Chinese Med.* 6: 111-126, 1995.
41. Markova, E.V., Obukhova, L.A. and Kolosova, N.G. Activity of cell immune response and open field behavior in Wistar and OXYS rats. *Bull. Exp. Biol. Med.* 136: 377-379, 2003.
42. Markovets, A.M., Saprunova, V.B., Zhdankina, A.A., Fursova, A., Bakeeva, L.E. and Kolosova, N.G. Alterations of retinal pigment epithelium cause AMD-like retinopathy in senescence-accelerated OXYS rats. *Aging (Albany NY)* 3: 44-54, 2010.
43. Montoya, M.J., Giner, M., Miranda, C., Vazquez, M.A., Caeiro, J.R., Guede, D. and Perez-Cano, R. Microstructural trabecular bone from patients with osteoporotic hip fracture or osteoarthritis: Its

- relationship with bone mineral density and bone remodelling markers. *Maturitas* 79: 299-305, 2014.
44. Muraleva, N.A., Sadovoi, M.A. and Kolosova, N.G. The features of development of osteoporosis in senescence-accelerated OXYS rats. *Adv. Gerontol.* 1: 171-178, 2011.
  45. Obukhova, L.A., Skulachev, V.P. and Kolosova, N.G. Mitochondria-targeted antioxidant SkQ1 inhibits age-dependent involution of the thymus in normal and senescence-prone rats. *Aging (Albany NY)* 1: 389-401, 2009.
  46. Olanow, C.W. A radical hypothesis for neurodegeneration. *Trends. Neurosci.* 16: 439-444, 1993.
  47. Rajalingam, K., Sugunadevi, G., Vijayaananand, M.A., Sathiyapriya, J., Sivakumar, K. and Suresh, K. Anticlastogenic effect of diosgenin on 7,12-dimethylbenz(a)anthracene treated experimental animals. *Toxicol. Mech. Methods* 23: 77-85, 2013.
  48. Reagan-Shaw, S., Nihal, M. and Ahmad, N. Dose translation from animal to human studies revisited. *FASEB J.* 22: 659-661, 2007.
  49. Rosenkranz, G., Djerassi, C., Yashin, R. and Pataki, J. Cortical hormones from allsteroids: synthesis of cortisone from Reichstein's compound D (Abstract). *Nature* 168: 28, 1951.
  50. Salganik, R.I., Shabalina, I.G., Solovyova, N.A., Kolosova, N.G., Solovyov, V.N. and Kolpakov, A.R. Impairment of respiratory functions in mitochondria of rats with an inherited hyperproduction of free radicals. *Biochem. Biophys. Res. Commun.* 205: 180-185, 1994.
  51. Solovéva, N.A., Morozkova, T.S. and Salganik, R.I. Development of a rat subline with symptoms of hereditary galatosemia and study of its biochemical characteristics. *Genetika* 11: 63-71, 1975.
  52. Son, I.S., Kim, J.H., Sohn, H.Y., Son, K.H., Kim, J.S. and Kwon, C.S. Antioxidative and hypolipidemic effects of diosgenin, a steroidal saponin of yam (*Dioscorea* spp.), on high-cholesterol fed rats. *Biosci. Biotechnol. Biochem.* 71: 3063-3071, 2007.
  53. Stefanova, N.A., Fursova, A. and Kolosova, N.G. Behavioral effects induced by mitochondria-targeted antioxidant SkQ1 in Wistar and senescence-accelerated OXYS rats. *J. Alzheimers Dis.* 21: 479-491, 2010.
  54. Tada, Y., Kanda, N., Haratake, A., Tobiishi, M., Uchiwa, H. and Watanabe, S. Novel effects of diosgenin on skin aging. *Steroids* 74: 504-511, 2009.
  55. Tikhonova, M.A., Yu, C.H., Kolosova, N.G., Gerlinskaya, L.A., Maslennikova, S.O., Yudina, A.V., Amstislavskaya, T.G. and Ho, Y.J. Comparison of behavioral and biochemical deficits in rats with hereditary defined or d-galactose-induced accelerated senescence: evaluating the protective effects of diosgenin. *Pharmacol. Biochem. Behav.* 120: 7-16, 2014.
  56. Valko, M., Leibfritz, D., Moncol, J., Cronin, M.T., Mazur, M. and Telser, J. Free radicals and antioxidants in normal physiological functions and human disease. *Int. J. Biochem. Cell Biol.* 39: 44-84, 2007.
  57. Waarsing, J.H., Day, J.S., van der Linden, J.C., Ederveen, A.G., Spanjers, C., De Clerck, N., Sasov, A., Verhaar, J.A. and Weinans, H. Detecting and tracking local changes in the tibiae of individual rats: a novel method to analyse longitudinal *in vivo* micro-CT data. *Bone* 34: 163-169, 2004.
  58. Wu, J.S. and Chen, J.H. Clarification of the mechanical behaviour of spinal motion segments through a three-dimensional poroelastic mixed finite element model. *Med. Eng. Phys.* 18: 215-224, 1996.
  59. Wu, J.S.S., Lin, H.C., Hung, J.P. and Chen, J.H. Effects of bone mineral fraction and volume fraction on mechanical properties of cortical bone. *J. Med. Biol. Eng.* 26: 1-7, 2006.
  60. Wu, W.H., Liu, L.Y., Chung, C.J., Jou, H.J. and Wang, T.A. Estrogenic effect of yam ingestion in healthy postmenopausal women. *J. Am. Coll. Nutr.* 24: 235-243, 2005.
  61. Yin, J., Kouda, K., Tezuka, Y., Tran, Q.L., Miyahara, T., Chen, Y. and Kadota, S. Steroidal glycosides from the rhizomes of *dioscorea* spongiosa. *J. Nat. Prod.* 66: 646-650, 2003.
  62. Zhang, Y.B., Zhong, Z.M., Hou, G., Jiang, H. and Chen, J.T. Involvement of oxidative stress in age-related bone loss. *J. Surg. Res.* 169: e37-e42, 2011.
  63. Zhang, Z.B., Cai, C.Y., Tian, S.P., Li, M. and Zhuang, R.H. Lipid peroxidation affects serum T and Bcl-2 expression in the testis of aging male rats. *Zhonghua Nan Ke Xue* 13: 46-49, 2007 [In Chinese].
  64. Zhdankina, A.A., Fursova, A.Z., Logvinov, S.V. and Kolosova, N.G. Clinical and morphological characteristics of chorioretinal degeneration in early aging OXYS rats. *Bull. Exp. Biol. Med.* 146: 455-458, 2008.
  65. Zou, L., Bloebaum, R.D. and Bachus, K.N. Reproducibility of techniques using Archimedes' principle in measuring cancellous bone volume. *Med. Eng. Phys.* 19: 63-68, 1997.